# Polyacrylic Acid Macromolecule-Complexed Zinc Phosphate Crystal Conversion Coatings*

T. SUGAMA, L. E. KUKACKA, N. CARCIELLO, and J. B. WARREN,
*Process Sciences Division, Department of Applied Science, Brookhaven National Laboratory, Upton, New York 11973*

## Synopsis

When water-soluble polyacrylic acid (PAA) macromolecules are introduced into zinc phosphating liquids, significant improvements in the yield of conventional zinc phosphate conversion films deposited on carbon steel surfaces are obtained. The improvements include controllability of crystal dimensions, degree of crystallinity, and coating weight. The conversion layer formed is a composite microstructure consisting of a bulk PAA polymer and complexed PAA continuously overlaying a uniform array of fine dense zinc phosphate crystals. Interfacial studies of the composite layer using infrared spectroscopy, energy-dispersive X-ray spectrometry associated with scanning electron microscopy, and X-ray photoelectron spectroscopy indicated that the functional carboxylic acid groups in the PAA molecules were strongly chemisorbed by the Zn atoms at the outermost surface sites of the crystal layers. The intermolecular bridging action of the surface Zn atoms which connect the PAA and the zinc phosphate crystal layers results in good adhesion at the PAA-crystal interfaces. In addition, the plasticized complex formation plays an essential role in increasing the stiffness and the ductility of the normally conventional crystal films. The flexibility of the complex coating surface and the thickness and surface roughness of the thin PAA overlayer all affect the adhesive force at the interface between the organic polymer topcoat and the complexed coating.

## INTRODUCTION

Crystalline zinc phosphate depositions play an important industrial role in upgrading the corrosion resistance and coating adherence properties of ferrous or zinciferous (especially galvanized) surfaces. For carbon steel surfaces, the zinc phosphate modification can be accomplished by immersing steel plates in an oxidizing solution containing 9 parts zinc orthophosphate dihydrate and 91 parts 15% $H_3PO_4$. A well-crystallized zinc phosphate hydrate conversion film which can be expressed in terms of a triclinic hopeite is formed. The typical surface topography consists of a dendritic microstructure array of interlocking rectangular crystals of insoluble zinc phosphate.[1] Prolonged exposure of the metal surface to the phosphating liquid results in the formation of a thick layer of dense interlocking crystals having an open surface structure. The crystal structure was also found to be a primary factor in the degree of bonding of paint and resin coatings to the metal substrates. An increase in mechanical anchoring is obtained when the liquid resins can penetrate into the open surface microstructure and microfissures of the deposited films.

*This work was performed under the auspices of the U.S. Department of Energy under Contract No. DE-AC02-76CH00016, and supported by the U.S. Army Research Office Program MIPR-ARO-155-83.

Journal of Applied Polymer Science, Vol. 30, 4357-4384 (1985)
 CCC 0021-8995/85/114357-28$04.00

Chemical treatments can be used not only to increase the roughness of the metal surfaces, but also to modify the chemical composition. The latter is an important factor affecting the degree of chemical affinity for polymeric adhesives. In an earlier BNL study of interaction mechanisms at organic polymer–zinc phosphate crystal interfaces,[2] it was shown that the coordinated and crystallized $H_2O$ molecules existing at the outermost surface of the conversion film play an essential role in wetting by the liquid resins which have functional carboxylic acid groups in the molecules.

The chemical attraction of zinc phosphate to functional polymer is due to intermolecular reactions resulting from the formation of strong hydrogen bonds, COO—$H_2O$, between the carboxylate groups derived from carboxylic acid and the water molecules of hydration at the crystal surface sites. These interactions enhance the bonding force at the interface. The results from the BNL work also suggested that a large crystal surface area, corresponding to the presence of a plentiful supply of polar $H_2O$ groups on the outermost surface sites, is more strongly chemisorbed by the functional polymers than are those with smaller surface areas.

Zinc phosphate conversion coatings are considered to be effective in protecting metal surfaces from corrosion, and phosphating processes have been used for this purpose for decades. However, the coatings are often porous and, as a result, ineffective. To obtain effective corrosion protection, a post-treatment process in which the phosphated metal surface is rinsed with a solution containing at least one polymer or copolymer of polyvinyl phosphonic acid and/or acid derivatives was developed.[3] In this process, polymer and copolymer penetrating into the pores of the phosphate films during the rinsing procedure contribute to the protective value of the deposition film.

The crystal structure and film thickness play key rolls in restraining physical deformation failures of the metals. However, increased coating thickness results in increased brittleness, thereby enhancing the potential for failure during flexure or other deformation. Therefore, a thin uniform array of fine dense crystals which is flexible should yield the optimum protective coating.

Protective films for metals must resist weathering, high humidity, and corrosive environments. A patent by Goltz[4] indicates that a chemical treatment of phosphates and phosphonates which contained free alcoholic hydroxyl groups proved effective in significantly reducing crystal size and coating weight when used directly in the phosphate conversion film-forming baths as crystal refiners. The resulting films are flexible and corrosion-resistant, even though the deposition weight is reduced.

The crystal size and coating weight of zinc phosphate conversion films deposited on metal surfaces can also be controlled by the addition of polymeric additives to the conventional zinc phosphating liquid. One such system is a mixture of an addition copolymer of an unsaturated carboxylic acid and a selected ethylenic monomer.[5] If the molecular weight of the polymer is too high, it will be insoluble in the phosphating mixture. Therefore, the crystal size attained may be limited by the molecular weight of the polymer. From the above, it appears that a zinc phosphate hydrate film consisting of a continuous array of large surface area crystals will exhibit

maximum adherence to polymer topcoats and provide good corrosion protection for metal surfaces.

The incorporation of organic materials in the zinc phosphating liquid as a method for improving the stiffness, the flexibility, and the moisture permeability of crystalline films appears possible. As described in an earlier paper,[1] the proton-donating COOH groups in polyacrylic acid (PAA) which are expressed in terms of polyelectrolyte macromolecules undergo an icn-exchange reaction with the free metallic ions in an aqueous medium. The active high-valency metallic ions contribute to the formation of inter- and intramolecular crosslinking of the polyelectrolyte macromolecules due to the salt bridge structure which replaces two hydrogens in the COOH groups located in the pendent of PAA. The nature of the ion–polyanion reaction mechanism suggests that the addition of PAA with a molecular weight ranging from 90,000 to 250,000 may be very effective in controlling the deposited crystal size. When the polyelectrolyte macromolecules are added to the zinc phosphating liquids, it is assumed that acid-base and charge transfer interactions will occur between the COOH groups and the divalent Zn ions which are a major chemical component of the crystallized zinc phosphate hydrate films. The interacting Zn cation will complex up to six molecules of $H_2O$ in the form of an octahedral structure. This chemisorbing function of the COOH groups resulting from this complex formation may serve to restrict crystal growth.

The objective of the present paper is to examine how the polyelectrolyte macromolecule-containing zinc phosphate conversion crystal film, formed by treating the metal surface with the PAA-modified zinc phosphating liquid, contributes to the improvement in the controllability of crystal thickness, the wettability by liquid resin, and the adherent properties to polymeric topcoat systems. The presence of organic polymers in the conversion films is expected to result in a film which will act in a manner similar to a primer for conventional polymer topcoatings. Expected primer formations may display an ability to promote the bonding forces at the composite film–polymeric topcoat interfaces. The interesting fundamental elements addressed above were studied experimentally using X-ray photoelectron spectroscopy, internal reflection infrared spectrophotometry, X-ray powder diffractometry, scanning electron microscopy associated with energy-dispersive X-ray spectrometry, differential scanning calorimetry, contact angle analysis, and computerized Instron system measurements.

## EXPERIMENTAL

### Materials

The metal used in the experiments was nonresulfurized mild carbon steel consisting of 0.18–0.23% carbon, 0.3–0.6% manganese, 0.1–0.2% silicon, and $\leq$0.04% phosphorous. Fine crystalline polyacrylic acid (PAA) complexed zinc phosphate hydrate films were deposited onto the metal substrate surfaces. The zinc phosphating liquid consisted of 9 parts zinc orthophosphate dihydrate and 91 parts 15% $H_3PO_4$ and was modified by incorporating a PAA solution at concentrations ranging from 0 to 12.5% by weight of the

total phosphating solution. Commercial PAA, 25% solution in water, having an average molecular weight of 104,000, was supplied by Scientific Polymer Products, Inc. The viscosity and pH values for these modified solutions ranged from 18 to 30 cP and 1.86 to 1.90, respectively. The PAA–zinc phosphate composite conversion film was deposited on the metal substrates by immersing the metal for up to 20 h in the modified zinc phosphating solutions at 60°C. After depositing the composite conversion films, the substrates were left in a vacuum oven at 150°C for ~5 h to remove any moisture from the film surfaces, and to solidify the PAA macromolecule.

Commercial-grade furan (FR) 1001 resin coating, supplied by the Quaker Oats Co., was used to determine the paint adherence properties of the composite films deposited on the metal surfaces. This resin had a viscosity of 470 cP and a surface tension of 35.4 dyn/cm at 24°C. The condensation-type polymerization of the FR resin was initiated by the use of 4 wt % QuaCorr 2001 catalyst, which is an aromatic acid derivative. The gel time for a 200-g resin sample containing the initiator was ~15 min at 24°C.

## Measurements

The image analysis of surface microtopography, measurement of crystal thickness, and quantitative multielement analysis of subsurface composition for the chemically treated metal surfaces were conducted with an AMR 100-Å scanning electron microscopy associated with TN-2000 energy-dispersive X-ray spectrometry.

A Perkin-Elmer Model 257 spectrometer was used for internal reflection infrared (IR) spectroscopic analyses. To detect the presence of the functional organic polymers in the conversion complex films and to estimate the concentration, IR spectra were obtained for samples prepared in the form of KBr discs. The samples were powdered before mixing and grinding with KBr.

Quantitative elemental information and identification of chemical states at the surface of PAA–zinc phosphate composite crystal layers can be obtained on the basis of the peak heights, precise determination of bonding energies, and peak shapes deduced from X-ray photoelectron spectroscopy (XPS) analytical techniques. XPS spectra of sample surfaces were taken using a CLAM 100 Model 849 Spherical Analyzer operating in a vacuum of $10^{-8}$–$10^{-9}$ Torr. Measurements were made with Al K$\alpha$ x-ray.

X-ray powder diffraction (XRD) analyses were employed to identify the zinc phosphate compound layers deposited on the treated metal surface. To prepare the fine powder samples, the deposited oxide layers were removed by scraping the surfaces and were then ground to a size ~325 mesh (0.44 mm). The magnitude of the wetting force of the modified metal surfaces by furan resin coatings was measured using a Contact Angle Analyzer in a 60% RH and 24°C environment. All the data were determined within 30 s after drop application.

In the support of XRD data, a DuPont 910 Differential Scanning Calorimeter with a heating rate of 10°C $min^{-1}$ in $N_2$ gas was used to determine the thermal decompositions of the identified zinc phosphate compound phases.

The lap-shear tensile strength of metal-to-metal adhesives was determined in accordance with the modified ASTM method D-1002. Prior to overlapping between metal strips 50 mm long, 15 mm wide, and 2 mm thick, the 10 × 15 mm lap area was coated with the initiated furan adhesive. The thickness of the Instron machine operating at a crosshead speed of 0.5 mm/min. The bond strength values for the lap shear specimens are the maximum load at failure divided by the total bonding area of 150 $mm^2$.

## RESULTS AND DISCUSSION

### Deposition Weight and Thickness

The investigation to determine the ability of PAA polyelectrolyte macromolecules to decrease the quantity of crystalline zinc phosphate conversion deposits was conducted using the following test procedures: The aqueous PAA solutions in amounts ranging from 0 to 8.0% by weight of total zinc phosphating liquid were dissolved in the phosphating solution by stirring. The polished metal plates were then immersed for up to 20 h in the phosphating liquid with and without PAA at 60°C. Immediately after immersion, the plates were placed in a vacuum oven for 10 h at 130°C. The surface of the dried plate was then washed with acetone solvent to remove the multiple-layer PAA polymer coating from the deposition films and then rinsed with water. The deposition weight, expressed as $mg/cm^2$ of treated metal surface, was consequently determined by a method in which the conversion crystal film was removed by scraping the surface of a weighed plate, and the plate was reweighed.

The results from the above tests are given in Figure 1. The resultant weight vs. immersion time curves indicate that the coating weight produced from the PAA-modified phosphating or unmodified liquids tends to increase with soaking time. For the oxidizing solution without PAA, the coating weight after a 1 h phosphate treatment was increased by a factor of 2.7 by extending the immersion time to 20 h. As is evident from the figure, the coating weight can be reduced by adding PAA, and the amount seems to correlate directly with the PAA concentration. At a phosphating age of 20 h, the addition of 8% PAA solution produced a coating weight of 7.9 $mg/cm^2$. This is 30% less than the value obtained using a phosphating solution without PAA for the same period of time. Thus, the presence of PAA macromolecules in zinc phosphate treatment processes reduces the coating weight, which could be economically desirable.

To further clarify the effects of PAA macromolecules on the coating weight, the extent of the conversion crystal growth deposited on metal surfaces was assessed using scanning electron microscopy (SEM). This technique is particularly useful since, with the aid of a stereo receiver, the crystals can be viewed in 3-dimensional relief. Samples measuring 6 × 2 × 1 mm were used to determine the approximate thickness of the crystals produced by zinc phosphate treatment lasting 7 h. The specimens were prepared by cutting a center portion of a larger-size metal plate with a diamond wheel. The SEM examination was focused primarily on the edge view of sliced sections. Figure 2 shows SEM photomicrographs of crystalline films deposited on metal surfaces treated with PAA-modified and unmo-

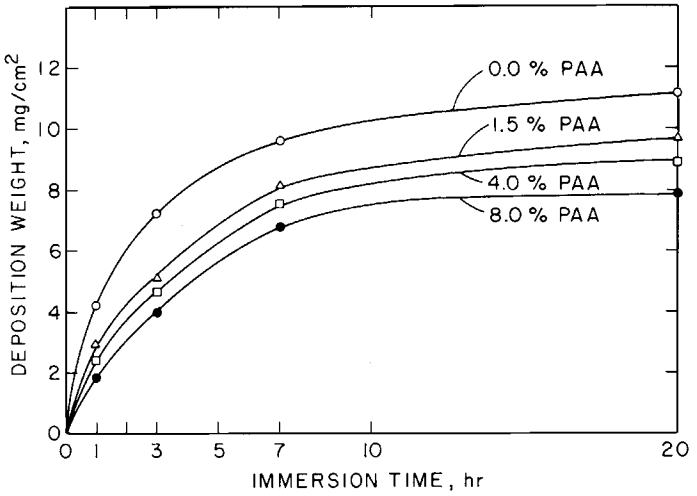


Fig. 1. Effect of PAA macromolecules on the coating weight of zinc phosphate deposition.

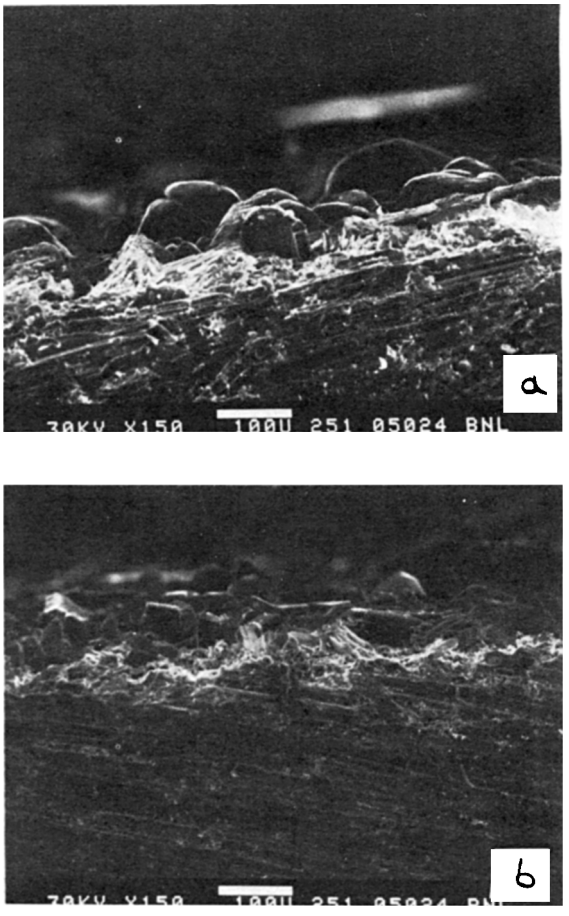


Fig. 2. SEM micrographs of edge views of zinc phosphate crystal sections: (a) metal surface treated with conventional phosphating solution; (b) surface produced with a 12.5% PAA-modified phosphating liquid.

dified phosphating liquids. The coarse crystals [Fig 2(a)] produced by immersing the metal substrate in the conventional phosphating liquid for 7 h were ~130 μm thick. In contrast, the coating deposited from a solution containing 12.5% PAA was considerably thinner and was comprised of relatively fine crystals [see Fig. 2(b)].

A curve of average crystal thickness as a function of PAA concentration was prepared by direct SEM observation of edge views in accordance with the procedures described above. This curve is shown in Figure 3. The zinc phosphate treatment time for all specimens used in this study was 7 h at 60°C. As is evident from the figure, the conversion crystal thickness decreases dramatically with an increase in the PAA concentration in the conventional phosphating liquid. Over a PAA concentration range from 0 to 12.5%, thickness varied between ~130 and ~60 μm. The presence of 12.5% PAA in the solution reduced the thickness to less than half that from the conventional liquid. The inclusion of 1.5% PAA reduced the thickness by 31%. Although not shown in the figure, it was not possible to deposit a coating on the metal substrate when 20% PAA was added. The reason for this was not evident. It is apparent that when water-soluble polyelectrolyte macromolecules having an average molecular weight of 104,000 are used as a deposition-reducing admixture, the concentration of the macromolecules in the phosphating liquid must be carefully estimated in order to produce a crystal film of the required thickness and coating weight.

The amount of the PAA polymer deposition on the metal substrate surfaces can be estimated by using IR absorption spectroscopy. Since the conversion of the PAA solution to a solid polymer is essentially completed during the process of drying the deposited film surfaces at 150°C, the powder

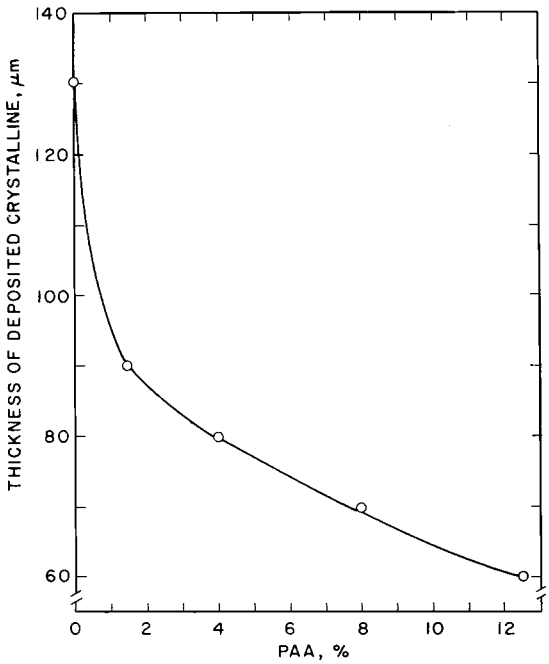


Fig. 3. Influence of the concentration of PAA solution on the deposited crystal thickness.

samples for IR studies were made by scraping the formed PAA–zinc phosphate composite crystal surfaces. IR spectra were then recorded for the samples prepared in the form of conventional KBr discs. The composition of the PAA-modified phosphating liquid was adjusted by varying the concentration of the PAA solution in the range of 0–12.5%.

The analytical work to compare the quantity of the deposited PAA polymers was focused on the changes in band intensity of the carbonyl C=O at 1710 $cm^{-1}$ and the CH of saturated methylene at 1440 $cm^{-1}$, which represent the pendent and main chain groups in the PAA polymer structure. Figure 4 shows the resultant IR spectra for these specimens over the frequency range of 1900–1300 $cm^{-1}$. Referring to the figure, the conspicuous band at 1630 $cm^{-1}$ for all specimens is assigned to the crystallized water of zinc phosphate hydrate films. Also, the intensities of the peaks at 1710 and 1440 $cm^{-1}$ gradually increase as the PAA concentration is increased. This implies that the quantity of PAA polymer deposited is directly proportional to the amount added to the phosphating liquids.

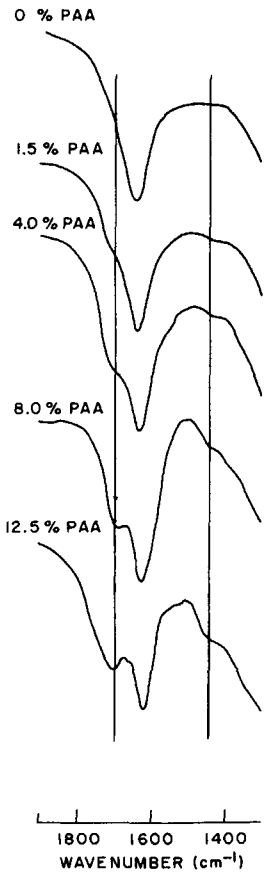


Fig. 4. Infrared spectra of zinc phosphate crystal films modified with PAA.

## SEM

The nature of the microtexture of the surface of the unmodified and the PAA-modified zinc phosphate crystal coatings was studied by use of scanning electron microscopy (SEM). Figure 5 shows electron micrographs of the surface microstructure of the deposition compounds prepared by soaking the metal substrate in the conventional and PAA-modified phosphating liquids for ~20 h. The conversion coating produced with the conventional liquid [see Fig. 5(a)] is characterized by the formation of a pronounced dendritic microstructure of triclinic zinc phosphate crystals. This morphological image indicates an interlocking structure of rectangular-like crystals which produces an extremely rough surface texture. In contrast, the metal specimens treated with PAA solutions had a much smoother surface. Figures 5(b) and (c) show microtexture views of 1.5 and 8.0% PAA-

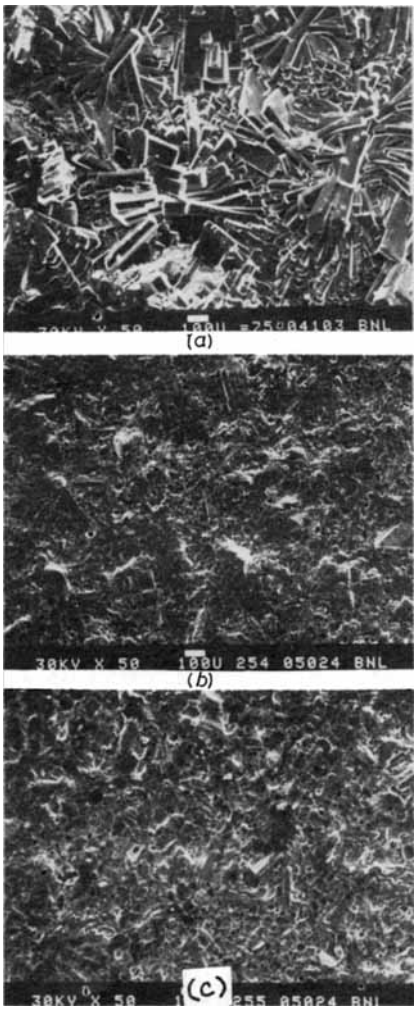


Fig. 5. Photomicrographs of metal surfaces treated with conventional and PAA-modified phosphating liquids: (a) 0% PAA; (b) 1.5% PAA; (c) 8.0% PAA.

treated metal surfaces, respectively. As seen in the photomicrographs, the topographical features were progressively changed from rough to smooth by increasing concentrations of the PAA solution. This is probably due to the multiple PAA polymer layers forming continuously on the surface of the conversion crystal film. However, the thickness of the overlaid PAA polymer films was not determined in this study.

It was presumed that the cured PAA polymers would produce a mechanically stable coating due to the formation of strong interlocking forces associated with the anchoring of the polymers into the open surface microstructure and microfissures of the crystal films, and the formation of chemical intermolecular attractions with the conversion zinc phosphate compounds. Detailed information regarding the latter will be discussed later in this paper. The thin PAA film formed on the crystals may also act to enhance the adherent properties of protective polymer topcoat systems because of the presence of functional carboxylic acid groups in the PAA molecular structure.

Since the PAA overlayers can be removed by rinsing with an organic solvent, considerable attention was given to the contrast between the surface topographical features of the conversion coatings after the PAA was removed. Metal surfaces used in the test series were treated with 0, 1.5, 4.0, and 12.5% PAA-modified phosphating liquids, and then washed with acetone to remove any PAA polymer, rinsed with water, and dried in a vacuum oven at 150°C. Resultant SEM photomicrographs are presented in Figure 6. Visual comparison of these micrographs shows the dimensions of the deposited crystals to decrease with increasing quantities of PAA in the

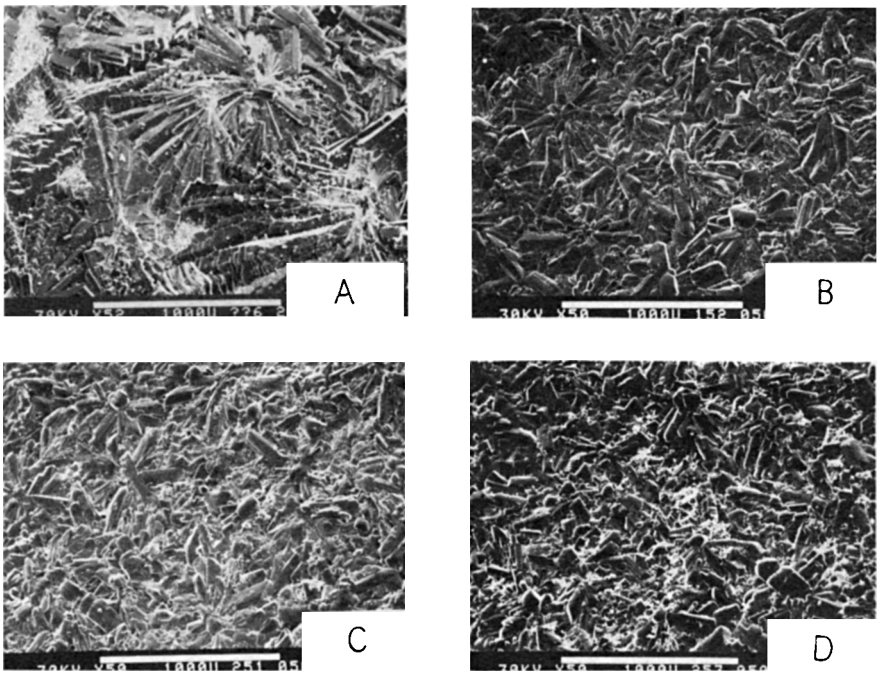


Fig. 6. Alteration in the conventional crystal size by PAA polyelectrolyte macromolecules: (a) 0% PAA; (b) 1.5% PAA; (c) 4.0% PAA; (d) 12.5% PAA.

conventional phosphating liquid. The micrograph of the conventional surface treatment [see Fig. 6(a)] indicates a dense agglomeration of rectangular-like crystals ~420 μm in length. Short rectangular-shaped crystals, ~320 μm in length, are produced by the addition of 1.5% PAA [Fig. 6(b)]. With 12.5% PAA, the crystal size is ~240 μm, ~43% smaller than the conventional crystal. Unfortunately, the reason for this is not evident. From the viewpoint of surface topographical features, examination further indicated that the uniformly configurated conventional zinc phosphate crystal is converted into randomly distributed fine crystals as the PAA concentration is increased. This may be due to the chemical transformations of the conventional crystals by polyelectrolyte macromolecules.

## EDX and XPS

The energy-dispersive X-ray (EDX) spectrometer coupled with SEM has a high potential for the quantitative analysis of any selected elements which exist at solid composite material subsurfaces. Its application can greatly enhance the results as well as facilitate the interpretation of SEM studies. EDX spectra for conventional zinc phosphate and 12.5% PAA-modified zinc phosphate composite film surfaces are shown in Figure 7. The abscissa of the spectrum is the X-ray energy characteristic of the element present, and the intensity of a gross peak count is related directly to the amount of each element present. As seen in the figure, it appears from the two strong peak intensities that the predominant elements in either the single or the composite conversion coatings are Zn and P atoms. Comparison of count rates for the Zn and P peaks indicates that there was more Zn in the coating system than P. Detailed information regarding the Zn-to-P count ratio as a function of PAA concentration will be discussed later. The spectra also exhibited a weak peak of Fe. The Fe is produced by the oxidation of metal surfaces. Since photoexcited EDX is useful for the elemental analysis of layers which are several micronthick, the Fe peak suggests that some Zn at distances up to several microns from the composite film surface is likely to be replaced by Fe.

Changes in the peak intensity of Fe by varying PAA concentrations are also of interest. In Figure 7(b) it is apparent that the Fe peak frequency for the 12.5% PAA composite layer is much stronger than for the conventional phosphate coating. Although not illustrated in the figure, the Fe frequency was observed to grow with an increasing PAA concentration. This implies that the thinner crystal deposition layers produced by incorporating large amounts of PAA solution consist of hybrid compounds of zinc and errous phosphate hydrates.

The EDX studies were also focused on the variation in Zn and P peak intensities for composite subsurfaces before and after rinsing with acetone solvent. Figure 8 illustrates EDX survey spectra for unrinsed and the acetone-rinsed 4.0% PAA composite subsurfaces. The spectrum for the untreated composite layer [Fig. 8(a)] is characterized by the conspicuous frequency of Zn which is the dominant element in this system. In contrast, the spectrum for the subsurface composite disclosed by removing the PAA macromolecular overlayer from the crystal surfaces [Fig. 8(b)] exhibited a noticeable transmutation, namely, the intensity of the Zn peak became

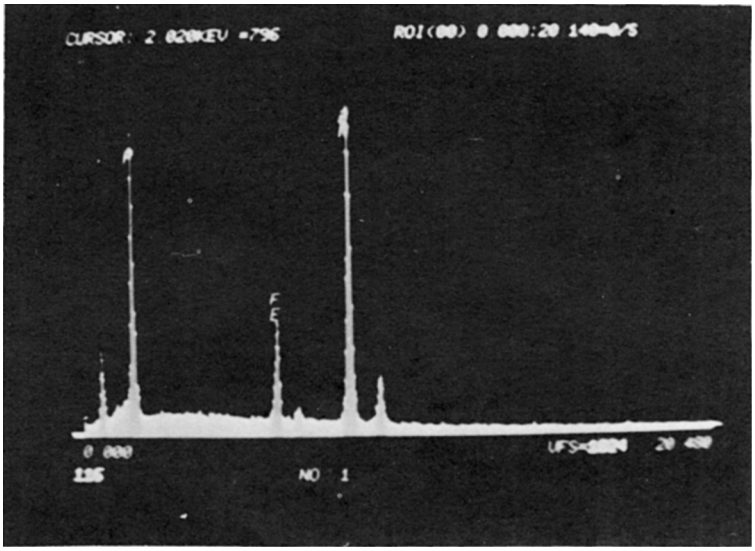


(a)

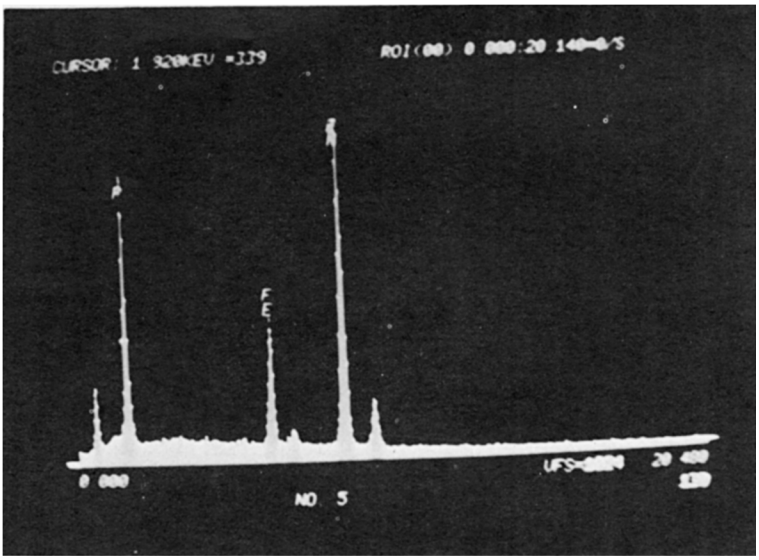


(b)

Fig. 7. EDX analysis of unmodified (a) and 12.5% PAA-modified zinc phosphate (b) conversion coating surfaces.

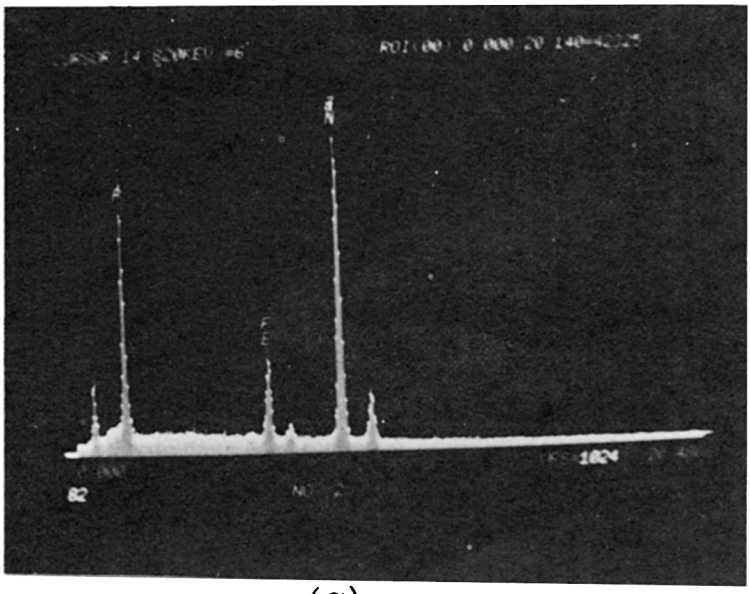


(a)

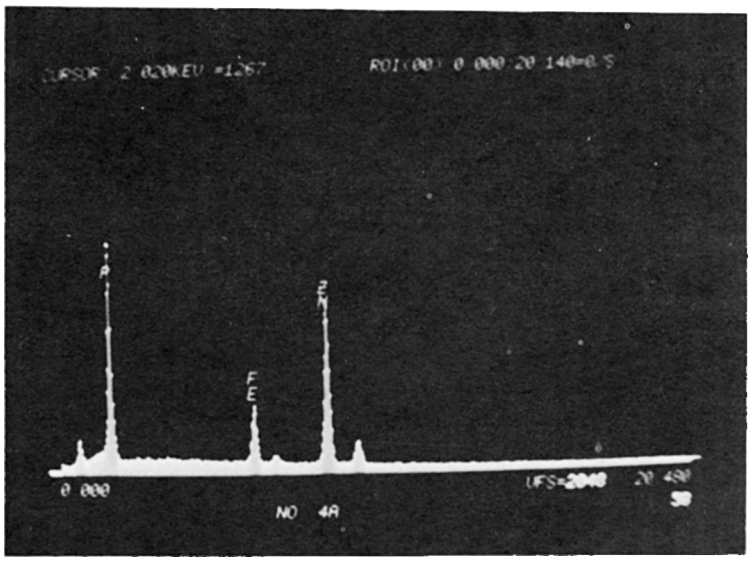


(b)

Fig. 8. EDX spectra of untreated (a) and acetone-treated 4.0% PAA-modified zinc phosphate composite coating surfaces (b).

much weaker compared to that of P. Even when smaller concentrations of PAA were used to modify the conventional zinc phosphate layers, similar spectral features were recorded for the acetone-treated composite coating subsurfaces. This surprising result seems to demonstrate that a certain amount of Zn is transferred to the interfacial contact layers of PAA macromolecules from the outermost zinc phosphate surface site. Hence, it was concluded that the transitional Zn element existing in the zinc phosphate molecular structure results in strong interfacial intermolecular attraction with the functional groups of PAA polymers.

The degree of the chemical attraction between the PAA and the Zn element can be quantitatively analyzed by comparing the ratio of Zn to P atom peak counts for the acetone-treated composite surfaces. An aim in the acetone treatment for the composite surfaces was to remove not only the bulk PAA polymer overlaid on the crystal surfaces, but also the PAA-based reaction products formed at the interface. For comparison purposes, Zn to P count ratios for untreated surfaces were also computed. These analytical results are listed in Table I. For the untreated composite layers, the data indicated that the Zn/P count ratio did not change very much with increased PAA concentration. Ratios ranged from 1.28 for the conventional zinc phosphate layers to 1.34 for 8% PAA-modified composite coating surfaces. In contrast, the Zn/P ratio values for the acetone-rinsed composite surfaces appear to be affected by the PAA content. As is evident from the table, the Zn/P ratios tend to decrease with an increase in PAA macromolecules. The value of 0.77 at 8.0% PAA is ~40% lower than that for samples without PAA. This correlation suggests that the polyelectrolyte macromolecules have a stronger chemical affinity for Zn than for P. Consequently, the Zn bound chemically to the PAA migrated as a result of the rinsing with acetone. From these observations, it can be speculated that when the polyacid is introduced into the zinc-phosphating liquid, an appreciable number of divalent Zn ions are preferentially taken up by the functional carboxylic acid (COOH) pendent groups in the PAA macromolecules which appear to act as a miniature ion–exchange system. The binding of the Zn ions may be essentially electrostatic in character, since ordinary equilibrium considerations cannot account for the binding quantitatively.[6] Hence, the reversible salt complex formation consisting of $COO^- Zn^{2+}$ coordinated

TABLE I
Ratio of Zn to P Atom EDX Gross Peak Counts for PAA–Zinc Phosphate Composite Films before and after Rinsing With Acetone

| PAA (%) | Zn/P ratio | |
|---|---|---|
| | Untreated composite layers | After rinsing with acetone |
| 0.0 | 1.28 | 1.28 |
| 1.5 | 1.39 | 0.87 |
| 4.0 | 1.30 | 0.81 |
| 8.0 | 1.34 | 0.77 |

groups could be obtained by a change transfer interaction between the carboxylate anions ($COO^-$) formed by the proton donor characteristics of the COOH groups and the active neucleophilic $Zn^{2+}$ ions dissociated from $Zn_3(PO_4)_2{\cdot}2H_2O$ in the phosphating solutions. The formation of the complex structure which involves intramolecular pairs of $COO^-$ groups associated with Zn ions in the zinc phosphate depositing stages may play a key role in restraining the conversion crystal growth, resulting in the production of a finely crystalline zinc phosphate deposition.

Accordingly, considerable attention was given to understanding the nature of the interaction at PAA–Zn interfaces during the transformation from a solution state to a solid conversion film. Assuming that the formation of the interfacial bonding is a local phenomenon involving only a few atom layers of PAA and Zn, a highly sensitive analysis technique such as X-ray photoelectron spectroscopy (XPS) was considered as appropriate for obtaining reliable information regarding the chemical interfacial interactions. XPS can be used to identify the chemical states and to obtain quantitative elemental analyses of thin surface layers ranging from 5 to 50 Å. Identifications can be made from precise determination of binding energies, peak shapes, and other spectral features. Quantitative analyses are made from XPS peak heights or areas. In our approach to the interface, it was considered desirable to investigate the interface before the occurrence of mechanically or chemically induced failure. Therefore, the surfaces of composite layers containing the PAA overlayers were studied to determine the nature of chemical interactions. Three coating surfaces, conventional zinc phosphate and 4.0 and 8.0% PAA-modified zinc phosphate, were employed in this test series.

Resultant XPS spectra indicated only four elements—Zn, P, O, and C—to be present on the composite coating surfaces. On the basis of the binding energies (eV) of their XPS lines, the chemical states of zinc and phosphorus are assigned to the crystalline zinc phosphate hydrate and carbon is attributed to the organic PAA polymers. Oxygen is present in both the crystal and PAA layers. The presence of Fe in the several-micron-thick crystal layer, which was clearly confirmed by EDX spectra, could not be identified on the XPS spectrum. This indicates that Fe atoms do not exist within 5 Å of the top surface of the composite coatings.

Figure 9 shows typical survey spectra of the zinc $2p_{1/2}$ and $2p_{3/2}$ core levels and illustrates differences in peak shape and peak intensity between unmodified and PAA-modified phosphate layers. The spectrum of the control surface is characterized by photoelectron peaks at two levels of adsorption in the binding energy ranges of 1048–1046 eV and 1024–1023 eV. It is of interest that these double peaks were shifted to single peaks by the incorporation of PAA. The spectra also show that the relative peak intensity tends to decrease with increasing PAA concentrations. In contrast, no significant changes in peak intensity and binding energy were observed from the phosphorus 2p core level spectra of the PAA–zinc phosphate system layers. This is shown in Figure 10. The phosphorus 2p peak shapes for 4 and 8% PAA-modified composite layers are quite similar to the peak shape of the control layer and have adsorption levels at ~135.5 and ~134.3 eV.

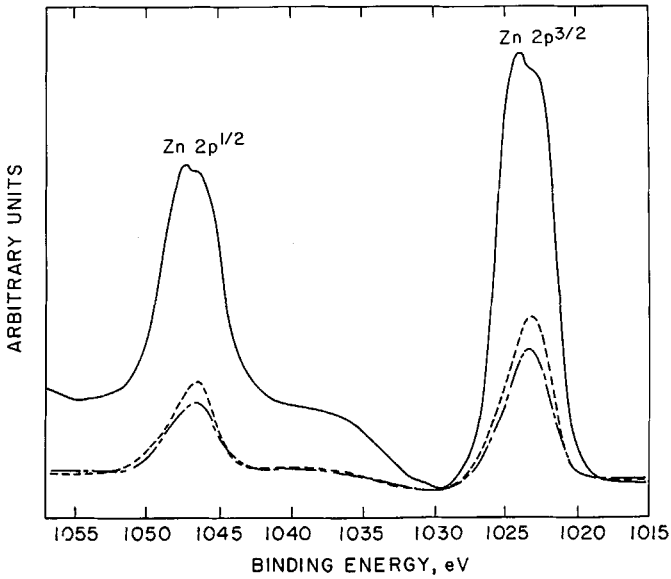


Fig. 9. Photoelectron spectra of Zn $2p^{1/2}$ and $2p^{3/2}$ in unmodified and PAA-modified zinc phosphate layers: (—) 0% PAA; (—) 4% PAA; (- - - -) 8% PAA.

These results clearly suggest that the functional PAA macromolecules are more strongly bound to the surface Zn atom rather than to an inert P atom. Figure 11 exhibits XPS signatures of oxygen 1S core levels. For the control layer, the peak at 532.9 eV assigns to the oxygen as P—O and Zn—O bonds. However, it is not yet clear whether it will be possible to distinguish the oxygen from either P—O or Zn—O. As is evident from the figure, the

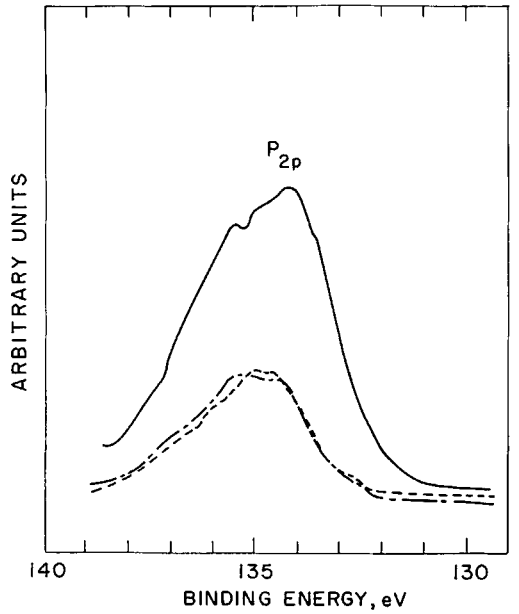


Fig. 10. $P_{2p}$ region of conversion coating surfaces: (—) 0% PAA; (—) 4% PAA; (- - - -) 8% PAA.

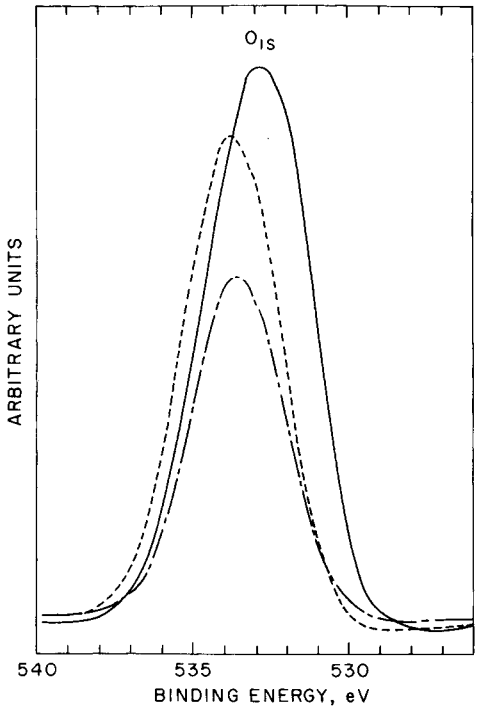


Fig. 11. Oxygen photoelectron peaks of (—) control, (- - - -) 4% PAA-, and (- - - -) 8% PAA-modified zinc phosphate film surfaces.

oxygen peaks associated with the presence of PAA are shifted slightly to higher in binding energies. The shifting peak was 0.8 eV higher than the control layer. This difference implies that the oxygen induced from the PAA-overlaid composite layers is related to that of COOH groups located in the pendent sites in the PAA molecular structure. For the $O_{1s}$ peak for the PAA composite layers, the peak intensity at 8% PAA is fairly weak compared to that for 4% PAA. This seems to suggest that the presence of a large number of COOH groups leads to a stronger chemical affinity for the zinc atoms.

The chemical accessibility of the COOH groups to the Zn atom can be established from the shift in binding energy of carbon 1S at ~290 eV which ascribes to the polar C=O groups. To obtain this information, two different PAA–zinc phosphate composite layers were used. One was a PAA–zinc phosphate crystal conversion film produced from a 1.5% PAA-modified phosphating mix liquid; the other was a PAA-coated crystal layer formed by means of vacuum vapor deposition of the PAA solution on a preformed phosphate crystal surface. The latter was prepared on the assumption that a strong chemical interaction at PAA–Zn atom interfaces would not occur. Two $C_{1s}$ spectra for these layers are illustrated in Figure 12. The spectrum for the PAA-coated layer exhibits a predominant peak at 284.9 eV and a minor peak at 289.8 eV. The former binding energy is associated with the characteristic alkane line contribution expressed in terms of the backbone carbon, and the latter reveals the C=O in the pendent COOH groups. When compared to the two peaks for the coated layer, conversion layer peaks are

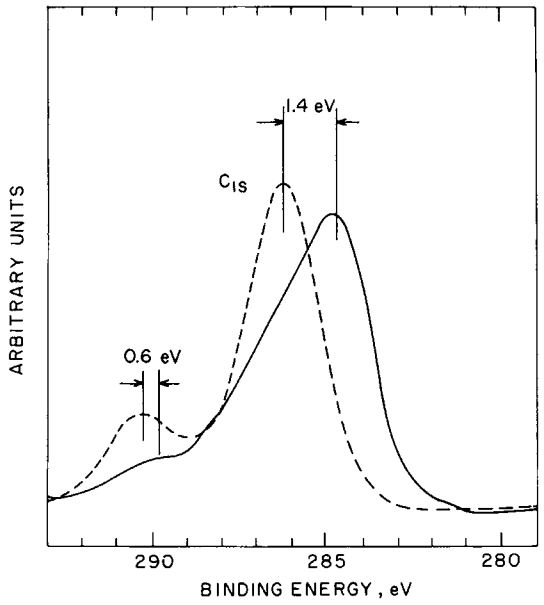


Fig. 12. Cis spectra from (—) PAA-coated and (- - -) PAA-modified zinc phosphate layers.

shifted significantly to a high binding energy. The difference between the binding energy values was 1.4 eV for the alkane line and 0.6 eV for the C=O. The figure also shows that the peak intensity of the alkane line for the conversion layer is approximately the same as for the coated layer. In contrast, it appears that the peak intensity of the C=O is considerably greater than for the coated layer. This change in peak shape and increase in binding energy is probably due to the strong accessibility of the functional side COOH groups to the metallic atoms. On the other hand, the strong increase in bonding energy of the alkane line for the conversion layer is likely to represent changes in conformation of the linear backbone chains which are assumed to be planar or zigzag.

From the results of the above EDX and XPS spectra analyses, it is speculated that the interfacial interaction between COOH and Zn which transforms the PAA–zinc phosphate solution into solid composite films is due to the following hypothetical mechanisms: the proton-donating functional COOH groups chemisorbed strongly with the Zn atom at the outermost surface sites of zinc phosphate crystal layers are converted into $COO^-$ anions. These anions induce strong ionic interactions associated with charge transfer bonding mechanisms. Subsequently, the converted $COO^-$ groups are transformed into unique bridge formations through a crosslinking reaction with Zn atoms. Hence, increased amounts of PAA will increase the degree of the crosslinking reaction. This also suggests that the chemical effect of the surface Zn atoms results in intermolecular bridging, which acts to connect the PAA macromolecular and the zinc phosphate layers. On the other hand, the newly formed COO—Zn bond may act to break the original zinc—oxygen bond in the zinc phosphate molecular structure. In fact, as confirmed from the EDX spectra analysis, the removal of Zn—complexed PAA macromolecules by rinsing with acetone solvent apparently

confirmed that the original Zn—O bonding force is much weaker than the COO—Zn bond. The tightly bound oxygen–phosphorus joint in the crystal molecules is likely to be unaffected by COO—Zn complex formations.

The reduction of Zn—O bonding forces caused by increasing PAA concentration was qualitatively interpreted using IR spectrometry. IR measurements were made on PAA-crosslinked zinc phosphate powder samples (size 0.04 mm) removed by scraping the substrate surface. The IR spectra for the samples prepared in the form of KBr discs were recorded in the range 1200–1000 $cm^{-1}$. The resultant IR spectra for all the zinc phosphate samples modified with up to 12.5% PAA were characterized by the presence of two conspicuous absorption bands. Table II presents the positions of the two bands obtained in this study. In the 1.5% PAA–zinc phosphate system, the first absorption band at 1110 $cm^{-1}$ would seem to be due to the P=O double bond, and the second band at 1030 $cm^{-1}$ is assigned to the stretching frequencies of $P—O^-$ groups.[7] As shown in the table, the positions of these two bands tend to shift to lower frequencies as the PAA content increases. It appears that the band shift is dependent on the PAA concentrations in the zinc phosphate hydrate. Even though the position of the Zn—O frequency is not detectable in the zinc phosphate compounds, it can be interpreted that such a pronounced shift of both the P=O and $P—O^-$ frequencies may be due to the reduction of the bonding energy between nonbridging oxygen ions and zinc ions in the P—O—Zn units. This implies that the extended PAA–Zn bonding force leads to a weaker Zn—O bond. However, the transformation mechanisms and conversion processes for PAA-crosslinked zinc phosphate layers from its solution state to a solid film are not evident from these limited data.

## XRD and DSC

Attempts to identify the crystalline conversion products of the PAA–zinc phosphate systems were made using X-ray powder diffraction (XRD) and differential scanning calorimetry (DSC). Both are reliable methods for detecting the constitution and alteration of deposition surface layers. XRD using Cu K$\alpha$ radiation at 50 kV and 16 mA and DSC at a heating rate of 10°C/min in $N_2$ gas were conducted on unmodified and 4% PAA-modified zinc phosphate powders.

XRD tracings recorded in the diffraction range 4.67–2.49 Å for powdered samples are given in Figure 13. For the control samples, the strong lines at 4.51 and 2.83 Å, the medium intensities at 3.44 and 3.36 Å, and the weak

TABLE II
Variation in Infrared Absorption Band Positions For Zinc Phosphate Compounds as a Function of PAA Content

| PAA (%) | Infrared absorption band positions ($cm^{-1}$) | |
|---|---|---|
| | P=O groups | $P—O^-$ groups |
| 1.5 | 1110 | 1030 |
| 4.0 | 1100 | 1025 |
| 8.0 | 1090 | 1020 |
| 12.5 | 1080 | 1010 |

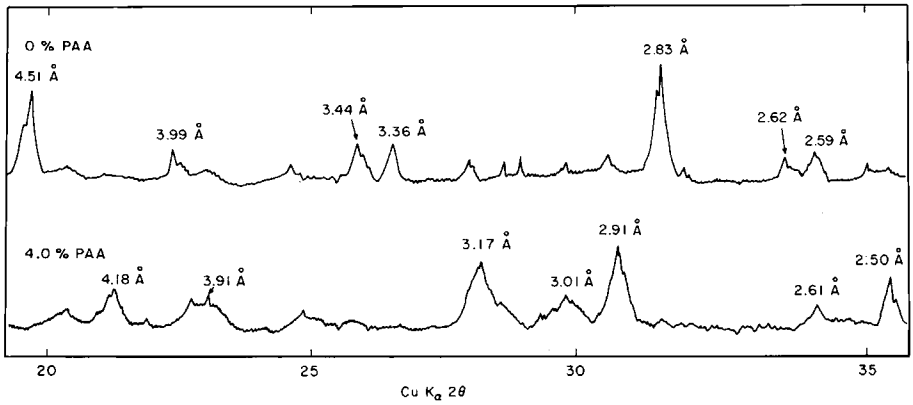


Fig. 13. Powder X-ray diffraction patterns of unmodified and 4.0% PAA-modified zinc phosphate crystal layers.

diffractions at 3.99, 2.62, and 2.59 Å are nearly identical to the XRD pattern for zinc orthophosphate hydrate. [$Zn_3(PO_4)_2 \cdot 4H_2O$] in terms of hopeite. Although the pattern shows other weaker lines which might represent some unidentified phosphate compounds, the major phase of crystalline conversion products yielded from the conventional zinc phosphating treatment is believed to be hopeite. In contrast, XRD patterns for the 4.0% PAA composite layer revealed quite different spacings, compared with those of the control. This suggests that the PAA leads to the transformation of the hopeite into the zinc phosphate compound phases having different chemical constituents and structures. The pattern in the limited diffraction regions seems to demonstrate that the transformed deposition layers consist of a hybrid phase of the ternary zinc phosphate-based hydration compounds. One of these compounds was identified as tertiary zinc orthophosphate dihydrate, $Zn_3(PO_4)_2 \cdot 2H_2O$, represented by the broad spacings at 3.17 and 2.91 Å and the small diffraction effects at 3.01, 2.61, and 2.50 Å. The presence of other unknown products is evident from the medium lines at 4.18 and 3.91 Å. However, a speculative mechanism for the transformation into the dihydrate-based zinc phosphate layers by the PAA is not clear at present. The role of Zn-complexed PAA macromolecules in transforming the conventional zinc phosphate molecular structures remains a subject for speculation and further research is required.

In support of the XRD data, typical DSC thermograms recorded as a function of temperature during the thermal decomposition of these samples are illustrated in Figure 14. The thermal measurements were performed in the temperature range 50–400°C. The thermogram for the control samples shows endothermic peaks at 80, 175, 225, and 235°C. The very slight endothermic peak at 80°C indicates a loss of moisture adsorbed on the sample surfaces. The prominent peak at 225°C, with an onset temperature of decomposition at ~175°C, is associated with the dehydration of the crystallized and coordinated water removed from the samples. The dehydration can also be recognized from an extreme reduction in the absorption intensity

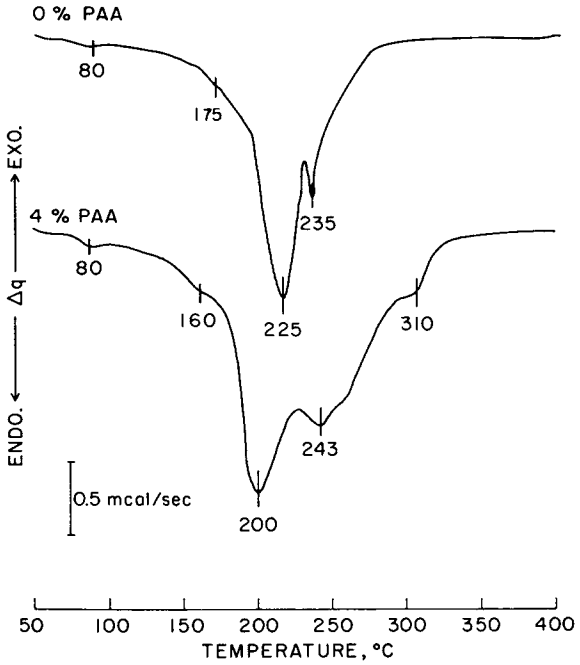


Fig. 14. Typical DSC thermograms for the control and 4% PAA-modified zinc phosphate hydrate crystals.

at 1630 $cm^{-1}$ frequency on the IR spectrum for samples heated to 225°C. The peak at 235°C may mean the approach to the end of the transition from the hydrated to the unhydrated zinc orthophosphate. On the other hand, the endothermal curve for PAA-complexed zinc phosphate layers indicates that the major thermal decomposition of the samples begins at ~160°C and the rate of decomposition rises to a maximum. This is followed by increasing decomposition heat which reaches a main peak at 200°C and subsequently leads to the generation of a new endothermal peak at 310°C. The latter may represent the temperature approaching the end of the transition phase. The temperature at this major peak corresponds to a 25°C reduction in the decomposition temperature, compared with that of the control. This shift is likely to be associated with a low degree of crystallinity of the zinc phosphate hydrate formed by the complex reaction with PAA. The conventional zinc layer is highly crystalline, which results in a brittle nonflexible material. The lower crystallinity of the PAA-modified films makes them more flexible. This is discussed in the next section. Consequently, the results from the XRD and DSC studies suggest that the addition of PAA to the conventional layers results in the assembly of hybrid zinc phosphate crystalline phases consisting of constituents and chemical structure different from those of the conventional film. Furthermore, the functional polyacid macromolecular acts to reduce the degree of crystallinity of the zinc phosphate hydrate deposited on the metal substrate surfaces and also leads to the production of finely crystallized coating layers.

## Flexural Stress–Strain Relations

The ductility and toughness properties of the crystalline conversion film itself are of considerable importance when the physical deformation characteristics of the metal substrates are considered. For instance, increased thickness of the deposition film layers makes the film increasingly brittle, thereby enhancing the potential for failure during flexure or other deformation. Generally, deformation failures of the layers having a low stiffness characteristic relate directly to the development of micropores and fissures which reduce the effectiveness of corrosion-resistant coatings.

In an attempt to evaluate the mechanical properties of the layers, the stress–strain relation and modulus of elasticity in flexure were determined using computerized Instron Flexure Testing Systems, operating at deflection rates of 0.5–0.05 mm/min. The determination of the stress–strain curve was made on the tensile zones of metal plate specimens, 6.2 cm long by 1.3 cm wide by 0.1 cm thick, subjected to three-point bending (see Fig. 15). As noted, the span was 5.0 cm. Figure 15 is a typical stress–strain diagram showing the control and 8% PAA-complexed zinc phosphate layers deposited on metal surfaces. The stress was computed assuming elastic behavior of the flexural member, and the strains were computed from the deflection measurements.

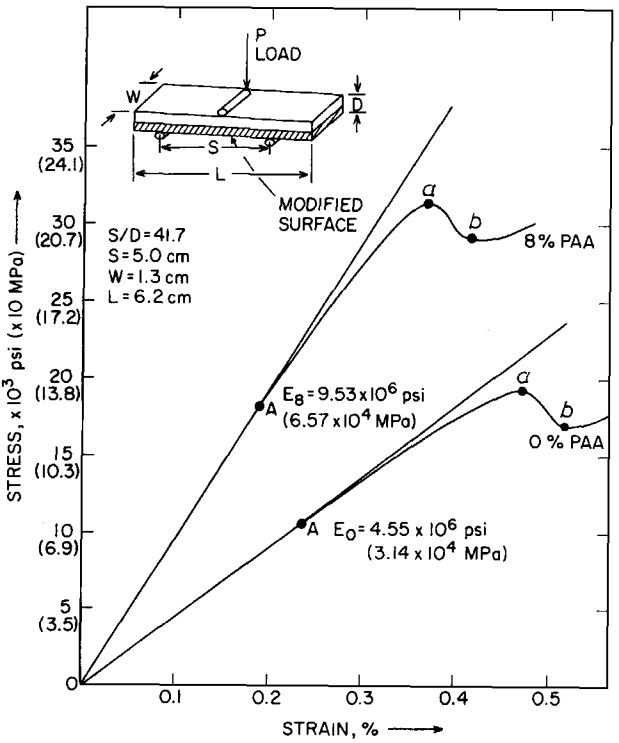


Fig. 15. Flexural load–strain curves for the control and 8% PAA-complexed zinc phosphate surface layers.

In the figure, the elastic region is the straight-line portion of the stress–strain curve from zero strain to the strain at point *A*. The elastic behavior implies the absence of any permanent deformation, so that point *A* is termed the proportional limit of the material. The slope of the line from the origin to *A* is the elastic modulus *E*. Physically, *E* represents the stiffness of the material to an imposed load. The resultant flexural modulus for PAA-complexed layers was computed to be $9.53 \times 10^6$ psi ($6.57 \times 10^4$ MPa), corresponding to a value twice that of the control specimens. This suggests that the stiffness of conventional crystal layers can be improved significantly by the incorporation of PAA.

The stress associated with the yield point of a layer is represented by the position of the line *ab* in Figure 15. The flexural stress at the yield point for the control was increased by a factor of 1.7 by adding an 8% concentration of PAA. Although not shown in this figure, the stress of the complexed layer during yielding increased somewhat with an extended strain, and an ultimate stress of $33.6 \times 10^3$ psi (232 MPa) was obtained at 1.08% strain. Further increases in strain resulted in the stress reduction. In contrast, the control exhibited no increase in stress after the onset of yielding deformation was noted. The deformation takes place at an essentially constant stress of $19.2 \times 10^3$ psi (132 MPa) until the stress reduction occurs around 0.75% strain.

The magnitude of the relative toughness of the materials can be obtained from the stress–strain curves by measuring the total area under the curves by drawing perpendicular lines from the ends of the curves to the strain coordinates. The area for the complex specimens was considerably greater than that for the control specimens. This apparently verifies that the deformation nature of the conventional crystal deposition can be made a more ductile one by the formation of a complex structure with PAA macromolecules.

From the above results, progressive failure of a control layer will occur following the development of an initial microcrack under applied local stress. However, when the conventional crystal layer is modified with polyelectrolyte macromolecules, the complex formed tends significantly to arrest crack propagation. An interpretation of this is that the energy generated in propagation of a crack is absorbed by the plasticized crystal layers. The enhanced ductility of the deposition layers is due not only to the organic polymer–inorganic crystal complexes, but also to the formation of thin layers of finely arrayed crystals. Consequently, the high rate of energy absorption resulting from the complex conformation plays an essential role in increasing the stiffness and in increasing the ductility of the conventional crystal layers.

## Adherent Properties

The lap shear bond strength of metal-to-metal furan adhesives and the changes in contact angle of the conversion film surfaces by liquid furan resin were measured as a function of PAA concentration. Metal substrate surfaces treated by immersing polished metal plates in the phosphating

liquid at 60°C for 7 h were employed in this test series. The treated surfaces were then dried at 150°C before the polymeric topcoats were applied. The furan (FR) topcoating system, described previously in the section on materials, was used to evaluate adherent properties of the complex conversion coating surfaces.

Test results from these specimens are given in Figure 16. The bond strength for the control specimen was ~650 psi (4.48 MPa). This increased progressively upon the addition of PAA in the concentration range from 1.5 to 4.0%. With 4% PAA, the strength was ~1150 psi (7.92 MPa). Further PAA additions up to 8% had little effect. Beyond 8%, strength reductions occurred. The failure surfaces generated by the shear test were visually examined to obtain information regarding the failure mode and failure locus. Observations indicated that, although the furan topcoat delaminated from the rough crystal surfaces of the control, a considerable overlayer of topcoat remained on the crystal surfaces. This is probably due to the strong mechanical interlocking produced by anchoring of the topcoat as a result of FR penetration into the open spaces in the interlocked crystal layers. All of the complex specimens, except for the one containing 12.5% PAA, exhibited very rough surfaces which resulted in extensive plastic deformation characteristic of the cohesive failure through a polymer layer. Examination of the surface of the 12.5% PAA sample indicated that it was much smoother than the surfaces of the other specimens and the extent of plastic deformation was much less. This suggests that the failure may have been through a mixed mode of cohesive (in FR polymer) and adhesive (near FR/complex interface) failures.

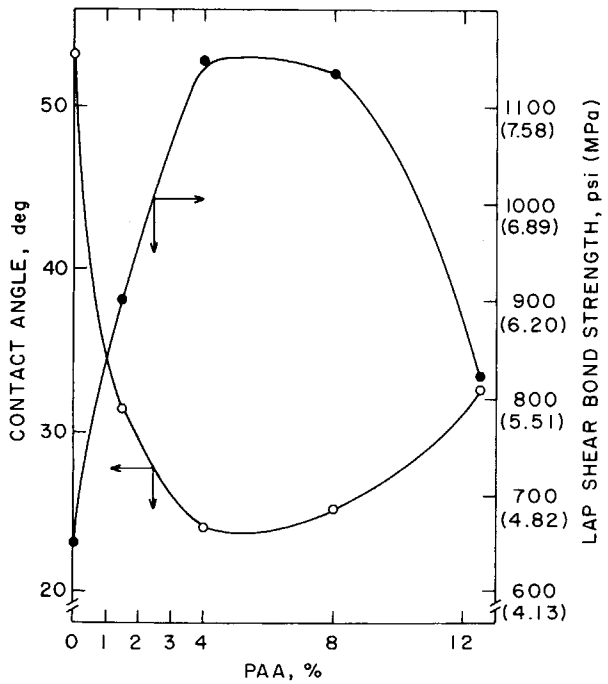


Fig. 16. Variation in contact angle and lap shear bond strength as a function of PAA concentration in complex conversion layers coated with furan.

The cohesive-type failure of the furan-complex layer during the shear bond test definitely indicated a well-made joint. This suggests that the surface of the complex conversion coating acts significantly as an adhesion promoter and primer to improve the adhesive bonding at FR/complex coating joints. Since the outermost surface sites of the complex conversion layers are occupied by a continuous thin film of PAA macromolecules, the functional carboxylic acid groups existing on the surface of the overlaying PAA must play a key role in developing chemical bonds between the two polymer materials. As addressed in many patents,[8–10] the bonding between the polymer substrate and the polymeric adhesive can be enhanced by the inclusion of carboxylic groups in the adhesive. This joint strength was found to be directly related to the interfacial chemical bonding between the carboxylic group and the polymer substrate. Thus, it is believed that the presence of a plentiful supply of COOH groups at the PAA surface sites results in increased chemical interactions at the polymer–polymer interfaces. In contrast, when the PAA concentration is lower, a very thin PAA overlayer having a relatively low number of COOH groups results in a poor chemical attraction for the topcoats. In this case, all available COOH groups at the overlayer site will be strongly chemisorbed by Zn atoms in the zinc phosphate molecular structure. Therefore, as a result of the neutralization of the functional groups, the Zn-crosslinked COOH will no longer have the ability to promote adhesion at the interface. Hence, the total number of functional groups remaining in the overlayer formed with a lower concentration of PAA is probably less than when a high PAA concentration is used. The molecular shape of a linear polymer 1000 atoms long in a rod ~1250 Å in length and 2.5–10 Å in diameter.[11] Thus, an ~20 Å minimum thickness of overlaying PAA macromolecules may be required for the development of the complex layer-to-polymeric topcoat adhesive strength. Conversely, the production of excessively thick PAA phase (concentrations >8%) will result in decreased bond strength. This can be explained if we understand wettability relationships between the liquid resin and the complex surface.

Experiments to obtain quantitative information regarding the magnitude of the wetting behavior were performed. In this work, the interfacial contact angle at the resin–complex film boundary was determined within 30 s after deposition of the liquid FR resin on the complex layers. The variations in contact angle plotted against the increasing PAA concentration are illustrated in Figure 16, where the two curves show an interesting correlation between the shear bond strength and the contact angle. The latter decreases and the bond strength increases for PAA concentration up to 4%. The contact angle increases and the strength decreases at higher PAA concentrations. The contact angle value for 4.0% PAA complex surfaces was significantly lower than for the control surface (20.8° vs. 53.1°). Since a lower contact angle results in an increase in the magnitude of the wetting forces, the wettability of the complex films appears to be enhanced by the incorporation of PAA macromolecules. It was considered that the significant improvement in wettability of the complex surfaces caused by increasing PAA concentrations might be due to the presence of a plentiful supply of functional COOH groups on the overlaying PAA surfaces. The functional

COOH groups are accessible for chemical interaction to form a tightly bound polymer network with the polymer topcoat. This further suggests that a large PAA surface area, corresponding to the presence of an abundant number of COOH groups, is more strongly chemical bound by the resin than a smaller surface area. A possible interpretation for the facile resin mobility at liquid resin–PAA interfacial regions may be developed from the nature of primary covalent bond mechanisms. When a topcoating resin, initially in a liquid state, is brought into contact with the PAA overlayers, the liquid resin is mobile enough to migrate to the functional COOH group sites on the layer where the highly energetic chemisorption to form the covalent bonds is particularly favorable. Thus, the number of COOH groups is important in promoting mobility of the FR resin. On the other hand, when the PAA concentration was 12.5%, a contact angle of 32.6° was measured. This is ~57% higher than the value with 4% PAA. It was detected by SEM that the surface texture was much smoother than for the complex surfaces with lower PAA contents. This implies that, although the overlaying PAA thickness and the presence of functional COOH groups are important factors in the wettability of the complex film, the degree of the surface roughness of the layer also contributes. The relatively rough complex surface associated with a large PAA surface area interlocks with the topcoating systems to form a much stronger bond than would occur with a smooth complex surface. Once wettability is fully developed, the interface is cohesively diffused over a certain depth, and failure will occur through a weaker part of the bulk, namely, the FR.

Consequently, the thickness and surface roughness of the overlaying PAA were found to be significant factors affecting the enhancement in the interfacial bond strength of the topcoat/conversion coating joint. The results for the production of a complex film which will yield maximum adhesive strength with polymeric topcoats.

## CONCLUSIONS

Crystalline zinc phosphate conversion coatings deposited on carbon steel substrates by immersing the metals in nongassing phosphating solutions are generally thick (~130 μm) and are comprised of relatively coarse crystals. These crystal formations which consist of a pronounced dendritic microstructure result in a high coating weight which is economically undesirable. Although well-crystallized conversion coating plays a role in the development of strong mechanical interlocking bonds with polymeric topcoating systems, the deposition of a thick layer of coarse crystals resulted in the formation of brittle coatings which failed upon flexing. The undesirable characteristics of the conventional zinc phosphate crystal layers polyelectrolyte macromolecules having a molecular weight of 104,000, to the actual zinc phosphating liquid.

In particular, the dimensions and coating weight of the conventional conversion crystals decrease dramatically with increasing PAA concentrations. It is speculated that this grain-refining action of PAA is due to the following mechanism. When the polyacid is introduced into the zinc phosphating liquid, the active nucleophilic divalent zinc cations dissociate from the zinc orthophosphate dihydrate in an aqueous solution. These may pro-

duce reversible salt complex formations with functional carboxylic acid (COOH) pendent groups in the PAA molecular structure. The complexes appear to act as a miniature ion-exchange system. The formed complex structure may also play a key role in restraining the conversion crystal growth, thereby resulting in a uniform dense coating of fine crystal size and low coating weight. The microstructure of the PAA-modified zinc phosphate layers was confirmed to be a composite formation consisting of a thin PAA macromolecule overlaying continuously on a uniform array of fine dense crystals.

To study the interfacial interaction mechanisms between the PAA polymer and the zinc phosphate crystal layers, elemental analyses of the composite surfaces and subsurfaces were conducted by means of the highly sensitive analysis techniques such as XPS and EDX. These results suggested that the interaction at the interfaces is most likely chemical. The chemical interaction is initiated by charge transfer reaction mechanisms in which the proton-donating functional COOH groups in PAA are strongly chemisorbed to the Zn atom at the outermost surface sites of the crystal layers. The carboxylic anions converted from the COOH groups are terminatively transformed into unique bridge formations through a crosslinking reaction with Zn. Thus, the chemical effect of Zn atoms in the hypothetical interaction model was presumed to be intermolecular bridging, acting to connect between the PAA and the crystal phases. The deposition products of the PAA-complexed zinc phosphate crystal were identified to be the assemblage structure of hybrid phases consisting of the tertiary zinc orthophosphate dihydrate as the major product and some unidentified phosphate compounds as the minor ones. The assemblage of this fine crystal further suggested that the PAA significantly acts to reduce the degree of crystallinity of the zinc phosphate compounds, resulting in the production of finely crystallized coating layers.

On the other hand, the plasticized complex coating layer plays an essential role in increasing the stiffness and the ductility of the conventional crystal layers. The flexural modulus of $9.53 \times 10^6$ psi ($6.57 \times 10^4$ MPa) for the 8% PAA-complexed layers corresponds to an improvement of $\sim$ two times over that for the layers without PAA. The maximum strain for the control was increased by a factor of 1.4 by adding 8% PAA.

With regard to the adherent aspects of complexed coating surfaces, it was found that PAA films overlaid on fine crystal surfaces act significantly to promote adhesive bonding at organic polymer topcoat–complex coating joints. This was associated directly with the interfacial chemical bonding between the COOH groups and the polymer topcoat. The highly stable nature of the interphase region due to the strong chemical attraction results in a cohesive failure mode through the considerable overlayer of topcoat remaining on the complex surfaces. The adherent properties of overlaying PAA are due not only to the thickness of the PAA film, but also to the degree of the surface roughness. The relatively rough complex surface, associated with a large PAA surface area, resulted in a much stronger chemical bond than that obtained with a smooth complex surface formed by the addition of an excessive amount of PAA. Accordingly, 4.0% PAA is likely to be an optimum concentration to produce complex layers which yield maximum adhesive strength with polymeric topcoats.

We gratefully acknowledge Dr. M. I. Florit for abtaining the XPS spectra for the polymer-modified conversion coatings.

## References

1. T. Sugama, L. E. Kukacka, and N. Carciello, *J. Mater. Sci.*, **19**, 4045 (1984).
2. T. Sugama, L. E. Kukacka, N. Carciello, and J. B. Warren, *J. Appl. Polym. Sci.*, **30**, 2137 (1985).
3. W. Herlest et al., U.S. Pat. 3,197,039 (1965).
4. K. Goltz, U.S. Pat. 4,427,459 (1984).
5. A. R. Morrison, U.S. Pat. 3,837,928 (1974).
6. F. T. Wall and J. W. Drenan, *J. Polym. Sci.*, **7**, 83 (1951).
7. K. Nakamoto, *Infra-red Spectra of Inorganic and Co-ordination Compounds*, Wiley, New York, 1963.
8. W. B. Reynolds, U.S. Pat. 2,774,703 (1956).
9. J. P. Strasser and E. R. Dunn, U. S. Pat. 3,338,858 (1967).
10. J. G. Brodnyan, U.S. Pat. 3,516,897 (1970).
11. E. Bear, *Engineering Design for Plastics*, Reinhold, New York, (1964), p. 64.

Received December 7, 1984
Accepted February 7, 1985